VetCore Facility for Research
University of Veterinary Medicine Vienna
(Head: Ao. Univ.-Prof. Dr. med. vet. Dieter Klein)

VetImaging
(Head: Dr. rer. nat. Martin Glösmann)

Ocular anatomy and retinal histology of the alpine marmot (*Marmota marmota*)

Diploma thesis

University of Veterinary Medicine Vienna

submitted by

Juliana Maria Giselbrecht

Vienna, March 2020

Betreuer: Dr.rer.nat. Martin Glösmann

Gutachterin: Ao.Univ.-Prof. Dipl.ECVO Dr.med.vet. Barbara Nell

Table of contents

1. Introduction

1.1. Alpine marmot

The alpine marmot (*Marmota marmota*) is a member of the order Rodentia and the family Sciuridae with the prairie dogs (genus *Cynomys*) and the ground squirrels (genus *Spermophilus*) as well-known relatives. The genus *Marmota* includes six North American (*e.g.,* ground hog, *Marmota monax*) and eight Eurasian species (*e.g., Marmota marmota*) (Kruckenhauser et al. 1999).

The natural habitat of the alpine marmot is in high altitudes of up to 200 m above local timberline, from 800 to 3200 m above sea level.

The alpine marmot is strictly diurnal and mostly herbivorous (Arnold 1999a). Marmots hibernate from October to April (Arnold 1999b). In contrast to the solitary *M. monax, M. marmota* is highly social (Kruckenhauser et al. 1999), living in groups up to 20 individuals spending their life together in self-constructed burrows. Marmots enter their burrows at night but also during the day, to rest, escape unpleasant weather conditions (e.g., heavy rain, heat) or flee their predators. Main natural enemies are birds of prey (especially the golden eagle, *Aquila chrysaetos*) and foxes (red fox, *Vulpes vulpes*). (Arnold 1999a). .

Early detection of predators seems an important ability of marmots to survive as individuals as well as a group. When threatened, alpine marmots warn members of the colony by shrill whistles that are heard over long distances. The alarm call is apparently quite efficient, as predators are an almost negligible source of mortality, unlike winter (Arnold 1999a). Thus, good eyesight to sense distant objects should play an important role in the life of a marmot.

Little, however, is known about the visual capacities of the alpine marmot. Previous studies have described the marmot retina as a pure cone retina (Bornschein 1961, Duke-Elder 1958, Rochon-Duvigneaud 1930, Walls 1942). Yet contemporary methodology has found rods and cones in all mammalian species examined (Peichl 2005).

1.2. General retina features

The retina forms the inner layer of the eyeball and is divided in two parts, with the ora serrata as a demarcation, the non-visual retina (pars caeca retinae) with the ciliary and iridal part of the retina, and the optic part of the retina (pars optica retinae). The optic part of the retina lies posterior to the ora serrata and is responsible for the transduction of photic energy. It converts light into electrical signal in the photoreceptors, processes these signals by other retinal neurons and transmits them along the optic nerve to the visual centres of the brain (König et al. 2014).

The retina has eight layers. The designation of these layers, from the outside to the inside, is as follows: retinal pigment epithelium (RPE), inner and outer segments of the photoreceptors (PR), outer nuclear layer (ONL), outer plexiform layer (OPL), inner nuclear layer (INL), inner plexiform layer (IPL), ganglion cell layer (GCL), and nerve fibre layer (NFL) (König et al. 2014).

The retinal photoreceptors are of two types, rods and cones. Rods are more light-sensitive and therefore used for vision at low light levels (night vision). In contrast, cones which need higher light levels to operate are used for daylight vision. Furthermore, different cone cells can contain different visual pigments, and therefore enable color vision. The distribution of rods and cones varies remarkably across mammals, loosely correlating with the daily activity pattern (Peichl 2005).

Nocturnal mammals have a rod dominant retina with relatively fewer cones (0.5 % to 3 %). In contrast, diurnal mammals, show larger cone proportions of 8 % to 95 % (Ahnelt and Kolb 2000, Peichl et al. 2000).

Few diurnal species are known to have more cones than rods. Examples are the squirrels with about 85 % cones (Kryger et al. 1998), and the tree shrews with about 95 % (Müller and Peichl 1989)

So far, all mammals studied using modern techniques have turned out to possess a duplex retina (i.e., containing rods and cones) (Ahnelt and Kolb 2000, Peichl 2005). According to Wässle (2004) pure rod retinas do not exist, likely because circuitry postsynaptic to rod photoreceptors requires the cone pathway to relay information down to the optic nerve. It is

conceivable that there are pure cone retinas, but to the present day, there is no proof for that in any species (Peichl 2005).

1.3. Aim of the study

The aim of this study was to provide further data on the ocular anatomy of the alpine marmot and to determine whether indeed this species has a pure rod retina, using histologic and immunofluorescence labeling techniques.

2. Materials and Methods

2.1. Animals and tissue fixation

Seventeen alpine marmots were used for this study (for further information about the specimens compare ***Table 1***. *Fehler! Verweisquelle konnte nicht gefunden werden.*Five marmots (S0/17, S1/17, S2/17, S3/17, S4/17) were shot by a hunter in Vorarlberg (Austria) in 2017, six marmots (Z608/12, Z609/12, Z613/12, Z616/12, Z619/12, Z621/12) were collected from the area of the Großglockner (Salzburg/Kärnten, Austria) in 2012 and six marmots (A1, A2, A11, C24, C29, C32) in Graubünden (Switzerland) back in 1996.

Eyes were enucleated within five minutes after death, except for the marmots collected in the Großglockner area. Their eyes were enucleated one day after death. Following the enucleation, eyes were opened with an incision at the sclero-corneal rim and fixed in 4 % neutral buffered formalin (NBF) for 12 to 24 h. The eyes from the marmots from Switzerland had been stored in fixative for 21 years. After fixation, all tissue was washed in phosphate buffered saline (PBS, two changes) and the eyes were stored in PBS at 7 °C until further processing.

2.2. Eye measurements

The following eye measures were taken using a dissecting microscope and sliding calipers to 0.1 mm accuracy (***Fig. 1***): axial length (AL), equatorial diameter (ED), corneal diameter (CD), corneal thickness (CT), lens diameter (LD), lens thickness (LT). The the ratio of CD to ED (CD:ED) and the ratio of CD to AL (CD:AL) were calculated. Both ratios measure the corneal diameter relative to the size of the eye.
The CD:ED ratio is closely linked to the amount of light admittance at maximum pupil dilation and to retinal image size (Kirk 2004).

2.3. Tissue preparation for histological analyses

Histological analyses of the major structures of the eye and exemplary measurements (thickness of cornea, sclera, retina) were performed in two right eyes of two one-year-old female marmots from Bivio (specimens A1, A2), the two eyes of the adult male marmot from Schröcken (specimen S0/17), and the left eye of an adult male marmot from Schoppernau (specimen S4/17).

For paraffin sections, the eyes were cut into pieces measuring 1.0 by 0.5 cm. The tissues were dehydrated through a series of increasing alcohol concentrations (70 %, 96 %, 100 %) and embedded in paraffin. Sections (3 µm) were cut with a rotary microtome (ZEISS Hyrax M55, Carl Zeiss MicroImaging GmbH, Jena, Germany) and mounted on Superfrost Plus slides (Thermo Fisher Scientific). Sections were stained with hematoxylin and eosin (H&E) for general histological examination or Heidenhain's Azan trichrome stain, which is used for the differentiation of extracellular connective tissue fibres, especially the discrimination of collagen fibres and reticulum fibres. The stainings were performed based on standard protocols (Mulisch and Welsch 2015).

For cryosections, both eyes of the adult male from Schröcken (S0/17) were used. The eye was hemisectioned (divided in two halves), the retina was isolated and cut into pieces of 1.0 by 0.5 cm, which were cryoprotected in ascending sucrose solutions (10 %, 20 %, 30 % in PBS with 0,01 % sodium azide, NaN_3, for 1 h each), before embedding in Tissue-Tek O.C.T. Compound (Sakura Finetek GmbH, Staufen). The tissue was shock-frozen in liquid nitrogen-prechilled isopentane and stored at -18 °C until further use.

Retinal quadrants were sectioned vertically at a thickness of 14 µm with a cryotome (CryoStar™ NX70 Cryostat, ThermoFisher Scientific) and mounted on Superfrost Plus slides (ThermoFisher Scientific). After 1 h of air-drying, cryosections were immunostained as described below.

For the preparation of a retinal wholemount, the eye of one adult male from Schoppernau (S4/17, left eye) was used. The eye was hemisectioned and the anterior part of the eye (cornea, ciliary body and lens) was dissected. In the remaining eyecup, containing most of the retina, the vitreous body was carefully removed using forceps and surgical scissors and the retina was carefully separated from the underlying retinal pigment epithelium. The dorsoventral

orientation of the retina could be determined by the location and orientation of the optic nerve head. Some of the retinal pigment epithelium remained attached to the neuronal retina without detrimental influence on later examinations of the specimen. Except for the immunofluorescent labelling the wholemount was left undyed.

2.4. Immunofluorescent labelling of rhodopsin

To confirm the presence of rhodopsin in photoreceptors of the alpine marmot, we performed immunofluorescent labelling with a rhodopsin-specific antibody on retinal frozen sections and a wholemounted retina. Air-dried frozen sections were circled with a liquid blocker pen (Super PAP Pen Liquid Blocker) and washed in PBS (four changes, 5 min each) to remove the optimal cutting temperature (OCT) compound embedding medium. Non-specific binding sites were blocked in 3 % normal donkey serum (NDS), 0.01 % NaN_3, and 0.25 % Triton X-100, diluted in PBS (protein blocking serum, 60 min, room temperature, RT). Sections were then incubated with mouse monoclonal anti-rhodopsin (clone 1D4, Genetex, GTX25417, 1:1,000-1:16,000) diluted in PBS with 3 % NDS, 0.01 % NaN_3 and 0.25 % Triton X-100 (for 16 h, RT). The next day the primary antibody was washed off with PBS (four changes, 5 min each).

Next the sections were incubated in secondary antibody solution (donkey anti-mouse IgG conjugated with Alexa Fluor 647, 1:300, in protein blocking serum) for one hour at RT. After rinsing in PBS (two changes, 3 min each) some sections were incubated with 4,6-diamidino-2-phenylindole (DAPI) for ten minutes to label nuclei and reveal the general retinal layering, particularly the outer nuclear layer formed by the somata of the photoreceptors. Finally, the sections were coverslipped in an aqueous mounting medium (Aqua Poly/Mount Polysciences Inc., Warrington, PA, USA).

To detect rods in the retinal wholemount, the same rhodopsin antibody as for the cryosections was used. To enhance antibody penetration, the retinal halves were cryoprotected in ascending sucrose solutions (10 % sucrose in PBS/NaN_3 for one hour, 20 % sucrose in PBS/NaN_3 for one hour, 30 % sucrose in PBS/NaN_3 for 12 h) and the tissues shock frozen at -80 °C three times. Preincubation was performed in protein blocking solution for 1.5 h at RT. Then the retinas were incubated with mouse monoclonal anti-rhodopsin (1:4,000, in protein blocking serum on a

shaker for 18 h at RT). After washing off unbound primary antibody with PBS (four times, 15 min each), the wholemount was incubated in secondary antibody solution (donkey anti-mouse IgG conjugated with Alexa Fluor 488, 1:300, in protein blocking serum) for 3.5 hours. After thorough washing in PBS the hemiretinas were flattened onto slides (a slide with the photoreceptor side up and coverslipped using Aqua Poly/Mount as a mounting medium).

2.5. Documentation and analysis

Photographs of the enucleated eyes were taken with a Nikon D750 DSLR. The paraffin sections were examined with a bright field microscope (ZEISS Axio Imager Z2, Carl Zeiss MicroImaging GmbH, Jena, Germany) using 10X, 20X, 40X oil, and 63X oil objective lenses and digital images were acquired with an AxioCam HR camera (Carl Zeiss MicroImaging GmbH, Jena, Germany) attached to the microscope. The analysis of the acquired images was performed in ZEN Blue (Carl Zeiss MicroImaging GmbH, Jena, Germany). The immune-labelled specimens were analysed with the same microscope using differential interference contrast and epifluorescence contrast, detected with the appropriate filters for Alexa Fluor 488 and Alexa Fluor 647. For the figures, images were adjusted for brightness and contrast using ZEN Blue.

3. Results

3.1. General eye features

The eyes of the alpine marmot were positioned laterally and fixed deep in the caudally opened bony orbit.

The results of the eye measurements are summarized in ***Table 2***. In the adult animals the AL was 13.5 ± 0.32 mm (mean ± SD), the ED was 16.3 ± 0.17 mm, and the mean CD was 9.6 ± 0.31 mm. In the juvenile animals, the size of the eyeball was smaller with a mean AL of 12.3 ± 0.3 mm, the ED was 14.2 ± 0.21 mm, and the mean CD was 9.2 mm.

The CD:ED ratio was 0.59 ± 0.02 mm (mean ± SD) in the adult animals and 0.64 ± 0.02 mm in the measured juveniles. The CD:AL ratio was 0.71 ± 0.02 mm in the adult marmots and 0.75 ± 0.02 mm in juvenile animals.

3.2. Extraocular muscles

Altogether seven extraocular muscles were identified in the orbita of the marmot eye (***Fig. 2B, C***). There were four well developed straight muscles (Mm. recti bulbi), two oblique muscles (Mm. obliqui bulbi), and a rudimentary retractor muscle which enwrapped the optic nerve (M. retractor bulbi). All extraocular muscles had their origin in the periorbita. The four rectus muscles inserted at the equator of the bulbus. The dorsal oblique muscle inserted at the dorsal and front surface of the sclera. The ventral oblique muscle had its insertion at the ventral sclera. The cone shaped retractor muscle inserted at the posterior pole of the eyeball and was separated from the other muscles by intraorbital fat.

3.3. Sclera

The sclera, i.e. the external tunic of the eye (***Fig. 2B***), contributes to the shape of the eye, was mainly composed of interlaced collagen fibres. The sieve-like area in the sclera, where the

ganglion cell axons exit the eye to form the optic nerve, is called the lamina cribrosa. This lamina was also present in the alpine marmot (***Fig. 9A***).

Measurements of scleral thickness made in two alpine marmots (A1, A2) revealed that the ventral sclera was nearly twice as thick (0.19 mm) as the dorsal sclera (0.09 mm). In general, the examined marmots had a thinner sclera anteriorly, near the corneal limbus, than posteriorly, in the region of the lamina cribrosa.

The sclera of the alpine marmot was heavily pigmented from the sclero-corneal limbus to the bulbar conjunctiva (***Fig. 2B***).

3.4. Cornea

The cornea of the marmot showed the distinctive mammalian design (***Fig. 4B***). In the region of the corneal limbus the corneal epithelium was found noticeably pigmented (***Fig. 6***), with the amount of pigment decreasing from the limbus to the peripheral corneal epithelium.

To a small extent pigmentation was also found around the marginal cornea vascular arcades. While the chemical nature of the pigment could not be determined in this study, its appearance was distinctly melanin-like and the localization of the pigment granules appeared to be limited to the cytoplasm of the corneal epithelial cells. Histologically, the nuclei of the corneal epithelium appeared almost free of pigment (***Fig. 6***).

3.5. Iris and pupil

The iris, the most anterior segment of the vascular tunic, presented itself as a dark, homogenous, and flat ring located between the cornea and the lens (***Fig. 2D***), surrounding the pupil that had the shape of a horizontal oval (***Fig. 2A***). The posterior iris epithelium was heavily pigmented (***Fig. 4C***).

In the iris stroma, close to the pupillary margin, a sphincter muscle was clearly discernible (***Fig. 4C***). Myoepithelial cells, found more centrally and located in the anterior iris epithelium, were forming a dilator muscle (***Fig. 4C***).

3.6. Lens

The lens of the alpine marmot is shaped ellipsoid and biconvex. Its posterior surface was more convex than its anterior surface (***Fig. 3B***).

In the adult marmots, the lens had a LD of 6.35 ± 0.28 mm and the LT measured 4.33 ± 0.51 mm. In the juvenile marmots, the lenses were considerably smaller (***Fig. 2F***). Their mean LD was 5.33 ± 0.19 mm and the mean LT 3.00 ± 0.08 mm. The lens measurements are summarized in ***Table 2*****.**

Furthermore, the LD:ED ratio was 0.39 ± 0.02 mm for adult alpine marmots and 0.37 ± 0.02 mm for the juvenile animals. The LT:AL ratio in adult animals was 0.30 ± 0.03 mm. In juvenile animals, the ratio was 0.24 ± 0.02 mm.

In the histological section, the lens was covered by a lens capsule (capsula lentis) (***Fig. 5***). The anterior surface of the lens was lined by a simple cuboidal epithelium (epithelium lentis). The epithelial cells became taller approaching the equator. Beneath the capsule and near the equator a nuclear bow (***Fig. 5***) and elongated lens fibres (fibrae lentis) were present (***Fig. 5***). The lens capsule was thickest in the area of the lens equator (14.43 µm, single measurement). Towards the posterior surface the capsule became gradually thinner (6.9 µm, single measurement). The lens was fixed in the posterior segment of the eye at its lens capsule by zonula fibres (***Fig. 5***).

A prominent feature of the marmot lens was its intense yellow color (***Fig. 2E, F, 3***). This was observed in both fresh and fixed samples. For comparison ***Figure 2E*** shows the lens of an alpine marmot in contrast to the fully transparent lens of a mouse.

3.7. Tapetum lucidum

No tapetum lucidum could be detected in the choroid of the alpine marmot, neither macroscopically nor after examination of the H&E or Azan stained histological sections.

3.8. Optic nerve

The unmyelinated nerve fibres, consisting of the ganglion cell axons, formed the horizontally elongated optic nerve head (***Fig. 2G***). It was a thin, white, horizontal streak located dorsal to the optic axis.
The optic nerve had acquired its round shape shortly after passing through the lamina cribrosa but before passing through the optic foramen (***Fig. 9A***). The optic nerve was remarkably thick compared to the size of the eyeball.

3.9. General retina features

The retina is the innermost tunic of the eye bulb and can be divided in two parts, with the ora serrata as demarcation (***Fig. 2D***): the non-visual retina (pars caeca retinae) with the ciliary and iridal part of the retina, and the optic part of the retina (pars optica retinae) (König et al. 2014). Like in other mammals, the retina was composed of eight layers (***Fig. 8***).
The retina of the alpine marmot was asymmetric. Ventral to the optic nerve head the retina was 0.17 mm thick. Dorsal to the optic nerve head the retina measured 0.05 mm (***Fig. 9B, C***).
The inner nuclear layer and the ganglion cell layer were prominent (***Fig. 9C***).
Dorsal to the optic nerve the inner nuclear layer was three nuclei thick, ventral to the optic nerve it measured twelve rows of nuclei.
The RPE was found in close association with the choroid and consisted of a monolayer of cuboidal epithelial cells with long apical microvilli intertwining with the outer segments of the photoreceptors (***Fig. 10***). It should be pointed out, that the melanin granules were mainly found in the microvilli part of the RPE. The basal portion of the RPE cells containing the cell nuclei were only sparsely populated with pigment.

Numerous blood vessels could be seen in the retina of the marmot both in the histological sections and in the wholemount. The retinal blood vessels were located mainly in the ganglion cell layer and in the nerve fibre layer and showed a holangiotic distribution (***Fig. 7***), which is

typified by the presence of large blood vessels which originate in the region of the optic nerve head and spread over the entire retina (Schaepdrijvers et al. 1989). The major vessels entered the retina through the papilla of the optic nerve. Several large vessels emerged side by side and formed a vascular pattern as illustrated (***Fig. 7***). The dorsal part of the retina showed a fine vascular drawing. In contrast to the ventral part of the retina, no large vessels could be identified.

3.10. Cones and rods

Vertical histological sections clearly showed the somata of the photoreceptors in the ONL. Dorsal to the optic nerve the ONL was one to two nuclei thick, whereas the ventral ONL had three to four tiers of nuclei (***Fig. 8B, C***). It was not possible to differentiate rod photoreceptors from cone photoreceptors on the basis of the morphology and the location of their nuclei. In the unstained wholemount it was also not possible to differentiate between rods and cones, as ***Figure 10*** shows.

Rods were identified by their rhodopsin-immunoreactivity in vertical cryostat sections immunolabelled with a mouse monoclonal rhodopsin-specific antibody. ***Figure 11 A*** shows an example of one section where in the field of view four photoreceptors are clearly rhodopsin-positive. The rhodopsin label revealed the morphology of the entire receptors including the outer and inner segments, the soma, and the axon with the axon terminal. The rod somata were located in the inner part of the ONL. The majority of nuclei in the ONL were left unlabelled with the rhodopsin antibody (***Fig. 11A***). This demonstrates the presence of a rare rod population in the alpine marmots retina.

4. Discussion

The anatomical and histological features of the eye of the alpine marmot described in this study are remarkably similar to that of the woodchuck, *Marmota monax* (Bezuidenhout and Evans 2005, Kirk 2006) and several squirrels (for measurements compare Chou and Cullen 1984, Gur and Sivak 1979, Hughes 1977, Merriman et al. 2016, Kirk 2006).This is not surprising, taken the close phylogenetic relationship of these species. The different species within the Sciuridae, however, slightly differ in their ecology. One could speculate that this also concerns visual ecology and that the eye would show adaptations to different environmental demands. If so, the conducted analyses were not able to reveal data that would support this assumption.

For example, the number and the position of the extraocular muscles were exactly like observed in other mammals (Walls 1942). Previous studies have shown that the size of the cornea relative to the size of the eye (CD:AL ratio, CD:ED ratio, compare ***Table 2***) is an excellent indicator of the circadian activity pattern (Kirk 2004, 2006, Walls 1942). It is well known that the alpine marmot is a diurnal mammal (Arnold 1999a). Conforming to this it could be observed that the corneal diameter was smaller in relation to the eye size than in nocturnal species (a relatively larger corneal diameter indicates that an eye can or needs to capture relatively more light) (Kay and Kirk 2000, Kirk 2004, 2006, Walls 1942).

Comparing juvenile and adult animals it could be perceived that eye size in the alpine marmot increased with age. The higher standard deviation for the CD:ED and CD:AL ratios in the group of adult marmots can be explained by the different ages the specimens in this group. It is also possible that slight inaccuracies occurred during the measurements with the sliding caliper. The measurements also showed that lens size increases with eye size.

The eye of the alpine marmot showed a horizontally elongated pupil, which should expand the visual field especially along the horizontal meridian. This, in turn, may increase the overlap of the visual fields of both eyes (binocular overlap). As binocular overlap enables stereoscopic vision, a larger binocular field could enhance odds to detect distant predators (Walls 1942).

Alpine marmots, due to the high elevation of their habitat, are exposed to high amounts of solar radiation whenever they leave their burrows (Türk and Arnold 1988). Therefore, it is possible that their eye shows features that are adaptations to UV radiation.

The muscles of the iris, musculus sphincter pupillae and musculus dilatator pupillae, which constrict and dilate the pupil, respectively, are well discernible histologically. Their presence suggests that the alpine marmot can adapt to the different light intensities in its environment. This would help minimize the amount of incident light on the retina, and thus potential UV damage. Adaptation has not been studied in the alpine marmot but in several close relatives of the squirrel family (woodchuck, prairie dog, ground squirrel). These studies prove that they possess noticeable adaptive capabilities (Bezuidenhout and Evans 2005, Duke-Elder 1958, Meekins et al. 2016, Peichl 2005, Rochon-Duvigneaud 1930, Rodriguez-Ramos Fernandez and Dubielzig 2013, Walls 1942).

Another precaution to protect from UV damage could be the pigmentation of the peripheral corneal epithelium, which was observed in the histological sections of the eye. Pigmentation of the cornea, however, is also known from beavers (Cullen 2003), capybaras, and prairie dogs (Rodriguez-Ramos Fernandez and Dubielzig 2013), species that live at lower altitudes and therefore are exposed to harmful radiation to a lesser extent. It needs further research to clarify whether there are differences in the concentration of the corneal pigment between species and whether they correlate with the exposure to radiation. Also, the chemical properties of the pigment are currently unknown.

The lens of the alpine marmot is completely yellow. In some diurnal primates, sciurid rodents, tree shrews, and meerkats a very specific compound was identified to be responsible for the yellow color of the lens. The pigment absorbs ultraviolet radiation as well as some of the blue range of the spectrum to protect the eye from retinal light damage (Douglas and Jeffery 2014). Hains et al. (2006) showed, that the lens of the 13-lined ground squirrel (*Spermophilus tridecemlineatus*), which is also yellow, contains N-actetylated derivatives of kynurenine and 3-hydroxykynurenine as major UV filters.

In this study no experiments were performed to investigate the chemical nature of the pigment present in the marmot lens. The characteristic yellow color of the lens, however, was observed in both fixed and fresh lenses. Therefore, it can be ruled out that the yellow lens color is an artefact due to chemical fixation as has been observed in other mammals (Peichl et al. 2016). Walls (1942) stated that the function of the yellow pigment was to alleviate effects of chromatic aberration in the dioptric mechanism by absorbing blue light. He also pointed out, that ‘the unfocusable shortwave light scattered in the atmosphere, and responsible for the bluish cast of

distant mountains and for the blue of the sky, is cut out by a yellow filter', creating a sharper image.

No evidence for the presence of a tapetum lucidum was detected in the choroid of the alpine marmot, which is similar to the woodchuck but also several other mammals with a diurnal life style (Bezuidenhout and Evans 2005, Ollivier et al. 2004). The function of the tapetum is to increase retinal sensitivity by reflecting light back to the photoreceptor layer and thereby increase the visual sensitivity at low light levels (Ollivier et al. 2004). Because marmots are exposed to high light intensities most of their lives, they apparently do not need this type of light amplification.

The optic disc, a thin, horizontally oriented streak was located above the optic axis. This variation of the optic nerve disc is also seen in woodchucks (Bezuidenhout and Evans 2005), ground squirrels (Kuester et al. 2004, Merriman et al. 2016), including the 13-lined ground squirrel, and in prairie dogs (Rodriguez-Ramos Fernandez and Dubielzig 2013). In other vertebrates, it is constantly located close below the visual axis or even on it, in the centre of the fundus (Walls 1942). Since the optic nerve head is a blind spot in the visual field, it is important that it is small and located at the right place. In the alpine marmot the blind spot is a blind streak. Because it is placed at the upper part of the retina, vision of the sky, where the predators of the marmots circle, should be left unaffected. Walls (1942) argued that the stripe-shape makes the disc so slender that it takes out only insignificant parts of vertical lines and that it would need only a minimal eye or head movement to move any horizontal line off the disc, onto functional, neuronal retina.

The vascularization of the retina was holangiotic, which means that blood vessels extended from the horizontal optic disc and built a large vascular network in the nerve fibre and ganglion cell layer. Once more this type of vascular supply is identical to that of the squirrel (Duke-Elder 1958, Rodriguez-Ramos Fernandez and Dubielzig 2013).

In the alpine marmot the ventral retina was thicker than the dorsal retina. Hence, one can assume that the number of neurons (*e.g.*, photoreceptors, ganglion cells) is higher ventral to the optic disc. Since the retina requires a good blood circulation for its function, it makes sense that the vascular supply in the ventral parts is more pronounced.

Altogether the histological findings for the general retina features in the alpine marmot were comparable to other mammals (Walls 1942). Alike, the dorsoventral asymmetry in retinal

thickness is a feature found in the close relatives of the alpine marmot, the ground squirrels, the woodchucks, and the prairie dogs (Hollenberg and Bernstein 1966, Rodriguez-Ramos Fernandez and Dubielzig 2013).

During preparation of the retina it was difficult to separate the neuronal retina from the RPE. It is possible that the reason for this difficulties was a very tight interaction of the RPE with the photoreceptors. Histological examination confirmed that the RPE of the alpine marmot had well developed apical microvilli intertwining with tips of the rod and cone photoreceptor outer segments. This is similar to other diurnal species but not the case in nocturnal mammals like rats or mice (Feldman and Phillips 1984). Maybe a very strong cellular connection between photoreceptors and RPE is particularly important in diurnal mammals that rely on vision. Any detachment of the photoreceptors from the RPE, which supports the photoreceptors metabolically, may cause blindness (Bonilha et al. 2006). For alpine marmots, vision seems to be important for survival, and a tight cellular connection between photoreceptors and RPE is not surprising.

In the past, it was assumed that some mammals, including sciuridae (Ahnelt 1985, Arden and Tansley 1955, Long and Fisher 1983, Szél and Röhlich 1988, Walls 1942) have pure cone retinas. Nowadays, it is known that these species also have a minor population of rods. Studies that have addressed the distribution of photoreceptor types in mammals using opsin antibodies have clearly shown that rods are present in the cone dominant retina of the California ground squirrel (Kryger et al. 1998), of the tree shrew (a member of the mammalian order Scandentia, which comprises only a few species of diurnal, insectivore-like mammals) (Müller and Peichl 1989), and in the cone-rich retina of the agouti (a South American rodent related to the guinea pigs) (Rocha et al. 2009). So far, no mammal has been found lacking rods entirely (Peichl 2005). The question remained for the alpine marmot. Rochon-Duvigneaud (1930), Walls (1942), and Bornschein (1961) provided anatomical and physiological evidence that strongly suggested that the marmot retina is rod-free.

In this study, the data from classical histological overview staining appeared to confirm this. In the sections stained with hematoxylin and eosin or Azan trichrome it was not possible to distinguish between rods and cones based on morphological criteria. This was surprising because in other sciurid rodents, researchers could assign rod and cone type identity after careful analysis of the location, shape, and microstructure (chromatin pattern) of their nuclei in

the outer nuclear layer (Ahnelt 1985, Cohen 1964, Long and Fisher 1983, Szél and Röhlich 1988). For instance, the cell bodies of cones in the European ground squirrel were always situated directly below the external limiting membrane (Ahnelt 1985). In grey squirrel, ground squirrel, and prairie dogs, the rod nuclei were round, while those of the cones were oval or polygonal (West and Dowling 1975). In the California ground squirrel, rod nuclei have their heterochromatin in the central and basal portions of the nucleus, while cones have apical and basal chromatin (Long and Fisher 1983).

Because of the inconclusive histology, the next step of this study attempted to differentiate rods from cones using immunofluorescence staining and an antibody specifically detecting mammalian rhodopsin. That way it was possible to clearly identify rods in the retina of alpine marmots.

In conclusion, this study described and depicted anatomical and histological features of the eye of the alpine marmot. Among these, the thickness of the sclera, the pronounced pigmentation in the area of the limbus corneae, the heavily pigmented iris, the yellow coloration of the lens, the horizontal and streak-shaped papilla n. optici, and the asymmetry in retinal thickness of the retina were strikingly similar to the phylogenetically closely related ground squirrel.

The present study demonstrated, for the first time, that the retina of the alpine marmot is cone dominant but not rod free. It contains a minor but distinct population of rod photoreceptors, a finding which contradicts earlier anatomical and physiological studies. Further work will need to be done to analyse the fine structure of the retinal layers, the distribution and ratio of cone subtypes, rods, and ganglion cells to evaluate potential functional consequences particularly regarding spatial resolution and color vision capability of the alpine marmot’s eye.

5. Zusammenfassung

Das Alpenmurmeltier (*Marmota marmota*) zählt innerhalb der Nagetiere (Rodentia) zur Familie der Zieselverwandten (Sciuridae) und ist im alpinen Raum Österreichs, Deutschlands und der Schweiz weit verbreitet. Sciuride Nager sind in der Regel tagaktiv und zeichnen sich im Gegensatz zu muriden Nagern durch ihren besonders gut entwickelten Sehsinn und eine für Säugetiere unübliche, zapfendominierte Netzhaut aus.

Im Gegensatz zum Ziesel, dessen Augenbau und Sehsinn sehr gut erforscht sind, gibt es vom Alpenmurmeltier dazu nur spärliche Informationen aus wenigen älteren Studien. Ziel dieser Arbeit war es daher, Daten zur Anatomie und Histologie des Murmeltierauges, unter besonderer Berücksichtigung der Netzhaut, zu sammeln.

Das Auge des Alpenmurmeltieres zeigte sich in zahlreichen allgemeinen Merkmalen dem des Ziesels sehr ähnlich. Lediglich in der Größe des Augapfels und im Linsendurchmesser unterscheiden sich die beiden Nagetiere merklich voneinander. Der Augapfel des Murmeltiers ist um zirka ein Viertel größer als der des Ziesels, die Linse jedoch um ein Viertel kleiner im Vergleich zum Ziesel. Bei der besonders starken Pigmentierung der bulbären Konjunktiva, des sclero-cornealen Limbus, sowie der Iris und der deutlichen Gelbfärbung der Linse könnte es sich um Anpassungen des Murmeltierauges handeln, die die Netzhaut vor der stärkeren UV-Belastung in Höhenlagen schützen.

Der Sehnervenkopf, der den blinden Fleck der Netzhaut bildet, stellte sich, wie beim Ziesel, als horizontale und streifenförmige Papille dar. Er war im dorsalen Drittel der Netzhaut lokalisiert und teilte damit die Netzhaut in einen kleineren dorsalen und einen größeren ventralen Abschnitt. Damit ist die Projektion des dorsalen Gesichtsfeldes auf eine große, ventrale Netzhauthälfte möglich. Das Merkmal könnte eine generelle Anpassung der Sciuriden zur guten visuellen Wahrnehmung von Fressfeinden aus der Luft sein. Interessanterweise ist die Netzhaut dorsal der papilla nervi optici um ein Drittel dünner als ventral davon und im Bereich der Verlängerung der Sehachse. Die Netzhaut der Murmeltiere galt bislang als völlig stäbchenfrei. Diese Ansicht konnte in der vorliegenden Arbeit widerlegt werden. Mit Hilfe eines Antikörpers für Rhodopsin, dem Sehpigment der Stäbchenphotorezeptoren, wurde Rhodopsin in einer kleinen Population von Stäbchen in der sonst zapfendominierten Netzhaut des Murmeltieres nachgewiesen.

Damit entspricht der Augenbau des Alpenmurmeltieres in den erfassten Merkmalen weitgehend dem des gut untersuchten Ziesels. Es müssten weitere, quantitative Studien durchgeführt werden, um beurteilen zu können, ob das Auge des Alpenmurmeltiers an die im Hochgebirge erhöhte UV-Strahlenbelastung besonders gut angepasst ist.

6. Abstract

The alpine marmot (*Marmota marmota*) is a member of the order Rodentia and the family of the Sciuridae. It is widespread in the alpine region of Austria, Germany and Switzerland.
Sciurid rodents are usually diurnal and, in contrast to murid rodents, they are characterized by a particularly well-developed sense of sight and a cone-dominated retina. In contrast to the ground squirrel, whose eye structure and sense of sight are very well studied, there is only spare information on the alpine marmot from a few older studies. Therefore, the aim of this study was to collect data on the anatomy and histology of the alpine marmot's eye, with special emphasis on the retina.
The eye of the alpine marmot showed many general characteristics very similar to those of the ground squirrel. Only in the size of the eyeball and in the lens diameter the two rodents differed distinctly from each other. The eyeball of the alpine marmot is about a quarter larger than that of the ground squirrel, yet the lens is a quarter smaller. The particularly strong pigmentation of the bulbar conjunctiva, the sclero-corneal limbus, as well as the iris and the distinct yellow color of the lens could be adaptations of the marmot's eye to protect the retina from the stronger UV exposure at high altitudes. As in the ground squirrel, the optic nerve head, which forms the blind spot of the retina, presented itself as a horizontal and striped papilla. It was located in the dorsal third of the retina and thus divided the retina into a smaller dorsal and a larger ventral section. This allows the projection of the dorsal visual field onto a large, ventral half of the retina. The feature could be a general adaptation of the Sciuridae for good visual perception of aerial predators. Interestingly, the retina dorsal of the optic nerve head is one third thinner than ventral in the region of the extension of the visual axis.
The marmot retina was previously considered to be completely rod-free. This could be refuted in the present study. With the help of an antibody for rhodopsin, the visual pigment of the rod photoreceptors, was detected in a small population of rods in the otherwise cone-dominated retina of the marmot.
In conclusion, for the examined features the eye of the alpine marmot largely corresponds to that of the well-studied ground squirrel. Further quantitative studies would have to be carried out to assess whether the alpine marmot's eye is particularly well adapted to the increased UV exposure in the high mountains.

7. Figures and tables

Table 1 Specimen details

Specimen	Collection site	Collection date	Sex	Age*
A1	Bivio, (Graubünden, Switzerland); 1769 m	25.04.1996	male	1 year
A2			female	1 year
A11			female	4 years
C24	Avers, (Graubünden, Switzerland); 1960 m	27.04.1996	female	3 years
C29			male	3 years
C32			female	4 years
Z608/12	Großglockner Hochalpenstraße (Salzburg/Kärnten, Austria); 2504 m	18.09.2012	female	Adult
Z609/12			male	Juvenile
Z613/12			female	Adult
Z616/12			male	Adult
Z619/12			male	Adult
Z621/12			male	Juvenile
S0/17	Schröcken/Alp Batzen (Vorarlberg, Austria); 1500 m	04.09.2017	male	2-3 years
S1/17	Schoppernau/Schadona (Vorarlberg, Austria); 1700 m	15.09.2017	male	4 years
S2/17			male	4 years
S3/17			male	4 years
S4/17			male	4 years

*The age was estimated by wildlife biologists or hunters based on size and weight, wear of teeth, and color of fur. Marmots need about 3 years to reach adult size (Arnold 1999a).

Table 2 Ocular dimensions of juvenile and adult alpine marmots

Species	Specimen	Age, sex	AL (mm)	ED (mm)	CD (mm)	LD/LT (mm)	CD:ED	CD:AL	LD:ED	LT:AL
Marmota marmota	A11*	ad, m	14.0	16.1	10.2	6.6/4.6	0.63	0.73	0.41	0.33
	C24	ad, f	13.1	16.3	9.2	6.6/4.1	0.56	0.70	0.40	0.31
	C29*	ad, f	13.6	16.5	9.3		0.56	0.68		
	C32*	ad, f	13.7	16.3	9.8		0.60	0.72		
	Z608/12	ad, f	13.1	16.1	9.5	6.1/3.8	0.59	0.73	0.38	0.29
	Z616/12	ad, m	13.5	16.3	9.5		0.58	0.70		
	Z619/12	ad, m	13.8	16.6	9.6	5.8/3.6	0.58	0.70	0.35	0.26
	S1/17*	ad, m				6.6/4.8				
	S2/17*	ad, m				6.3/4.4				
	S3/17*	ad, m				6.5/4.4				
	S4/17*	ad, m				6.1/3.2				
	Mean / SD		**13.5 ± 0.32**	**16.3 ± 0.17**	**9.6 ± 0.31**	**6.35±0.28/ 4.33±0.51**	**0.59±0.02**	**0.71±0.02**	**0.39±0.02**	**0.30±0.03**
	A01	ju, f		14.1						
	A02	ju, f		14.4		5.8/3.0			0.40	
	Z609/12*	ju, m	12.0	14.5	9.2	5.3/3.1	0.63	0.77	0.37	0.26
	Z621/12*	ju, m	12.6	14.0	9.2	4.9/2.9	0.66	0.73	0.35	0.23

	Mean / SD		**12.3±0.3**	**14.3±0.21**	**9.2±0**	**5.3±0.19/ 3.0±0.08**	**0.64±0.02**	**0.75±0.02**	**0.37±0.02**	**0.24±0.02**
Literature data										
***Marmota monax*[a b]**			12.0[a], 12,1[b]	15.0[a], 12.4[b]	9.0[a], 7.5[b]	5.5[a]/4.5[a]	0.60[a], 0.61[b]	0.75[a], 0.62[b]	0.37[a]	0.38[a]
***Spermophilus citellus*[c,d]**			9.0[c]	10.5[c]	-	8.32[d]/2.8[c], 2.91[d]				
***Ictidomys mexicanus*[d]**			-	8.23	-	8.32/2.91				
***Ictidomys tridecemlineatus*[e,f,g]**			9.45[f], 8.6[g]	9.5[g]	6.0[g]	4.0[g]/2.95[e],2.91[f]	0.63	0.70[g]	0.42	0.31-0.34
***Glaucomys volans*[b]**			8.3	8.6	7.8		0.91	0.94		

AL = eye axial length; **ED** = eye equatorial diameter; **CD** = corneal diameter; **LD** = lens diameter; **LT** = lens thickness; **CD:ED** = relative corneal diameter with respect to the eye's equatorial diameter; **CD:AL** = relative corneal diameter with respect to the eye's axial length; **LD:ED** = relative lens diameter with respect to the eye's equatorial diameter; **LT:AL** = relative lens thickness with respect to the eye's AL. **ad** = adult; **ju** = juvenile; **m** = male; **f** = female. For the individuals indicated with an asterisk (*), the data are the means of the dimensions of both eyes. For comparison, published data for the woodchuck (*Marmota monax*) and other

sciurid rodents, the European ground squirrel (*Spermophilus citellus*), the Mexican ground squirrel (*Ictidomys mexicanus*), the thirteen-lined ground squirrel (*Ictidomys tridecemlineatus*), and the Southern flying squirrel (*Glaucomys volans*) are given.
The Southern flying squirrel is the only nocturnal species in this table. All other listed species are strictly diurnal.

[a] Bezuidenhout and Evans (2005); [b] Kirk (2006); [c] (Hughes (1977); [d] Gur and Sivak (1979) ; [e] Chou and Cullen (1984); [f] Merriman et al. (2016); [g] Measures for ED, CD, LD taken from Sussman et al. (2011) where Figure 1 shows a cross-sectional image of the eye of a ground squirrel made through the center of the pupil, along the optical axis.

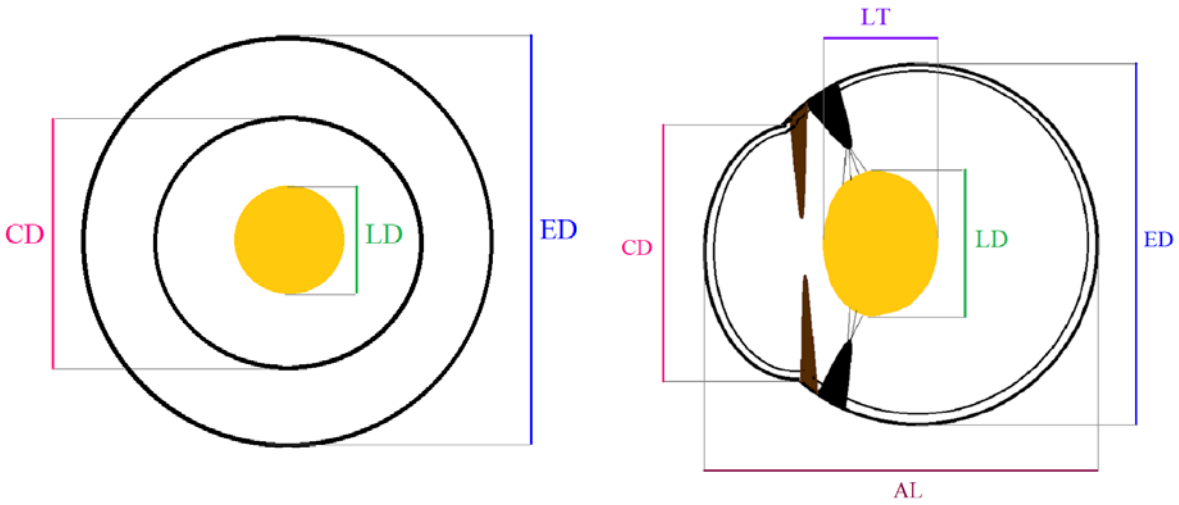

Figure 1 Schematic diagram of the measured eye parameters in this study

Left: frontal view of the eye. Right: Schematic sagittal section. CD, corneal diameter; ED, equatorial diameter; AL, axial length; LD, lens diameter; LT, lens thickness.

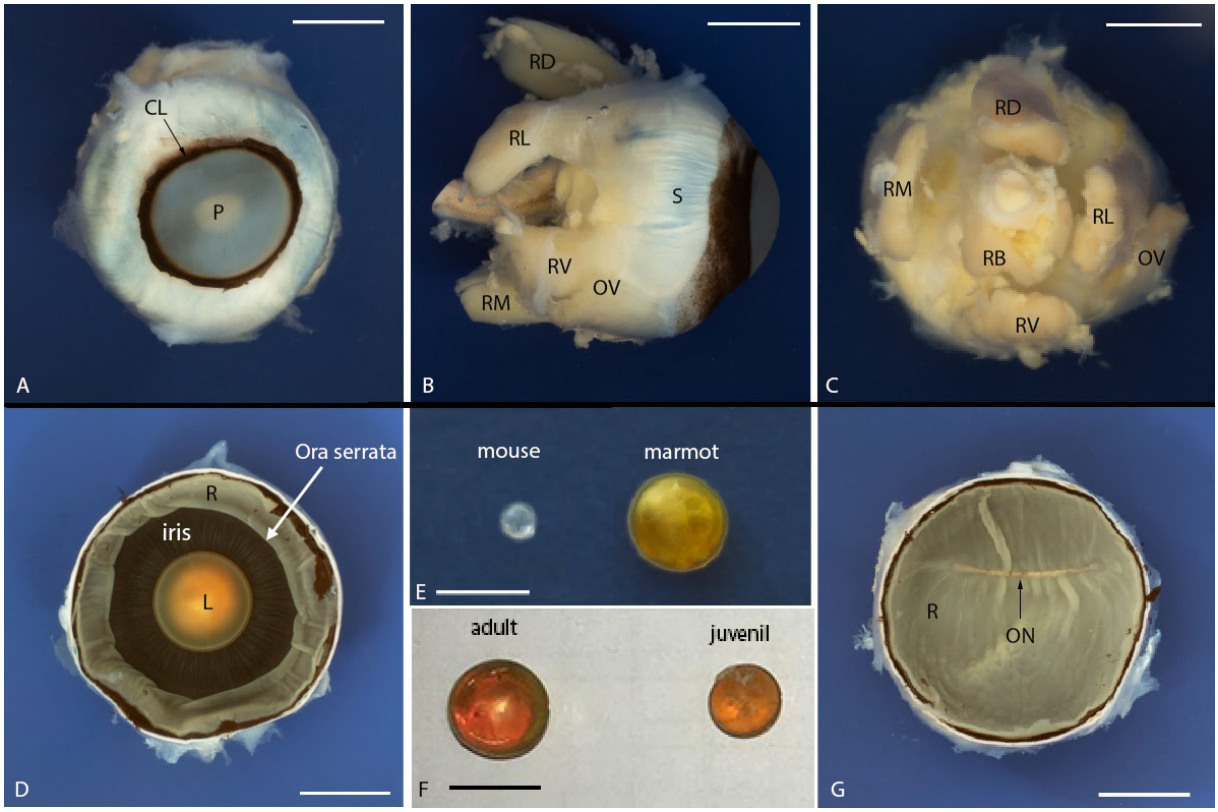

Figure 2 Macroscopic anatomy of the eye of the alpine marmot.

A, frontal view; B, lateral view; C, caudal view; D, equatorial cut, caudal view on the cranial part of the inner eye; E, comparison of a mouse's and marmot's lens; F, comparison of an adult and juvenile marmot's lens; G, equatorial cut, cranial view on the caudal part of the inner eye; CL, corneal limbus, P, pupil; RD, Musculus rectus dorsalis; RL, Musculus rectus lateralis; RV, Musculus rectus ventralis; RM, Musculus rectus medialis; OV, Musculus obliquus ventralis; S, sclera; RB, Musculus retractor bulbi; L, lens; R, retina; ON, optic nerve. Scale bar, 500 µm.

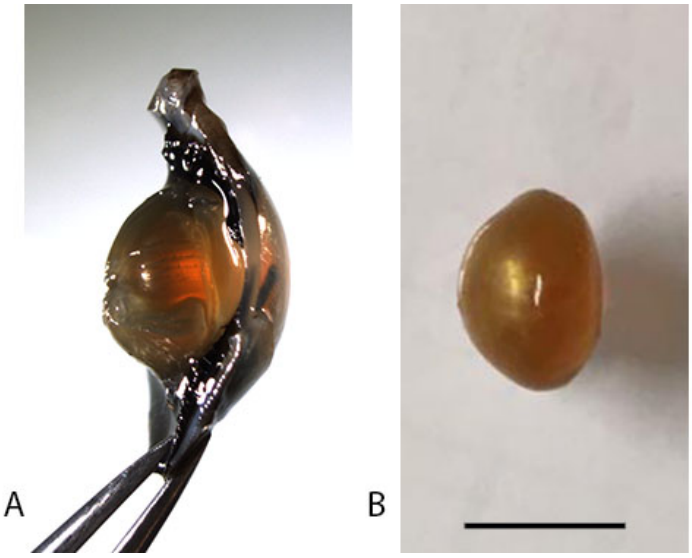

Figure 3 Lateral view of a lens of an adult alpine marmot

showing the different curvature of the front and rear surface of the lens. A, the lens is fixed in the posterior segment of the eye by zonula fibres. B, detached lens. The posterior surface of the marmot lens is more convex than the anterior surface. Scale bar, 500 µm.

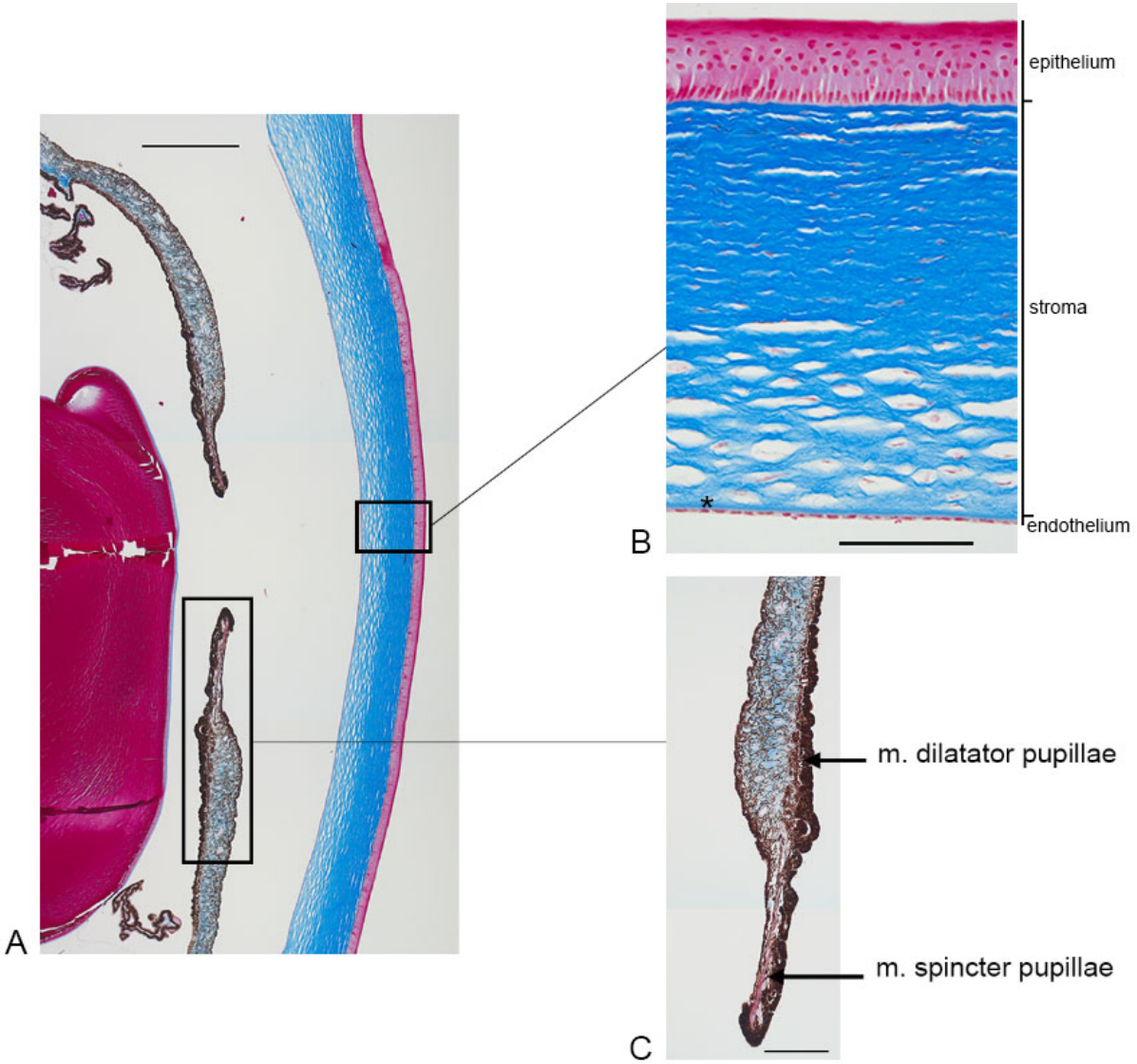

Figure 4 Microscopic structure of cornea and iris.

A, Azan stain of lens, iris, and cornea. Scale bar, 500 µm; **B**, Cross section of the cornea. The cornea consists of five layers. Multilayer squamous epithelium, thin Lamina limitans anterior, also known as the Bowman's membrane, the avascular and rich in collagen fibrils stroma and endothelium of the cornea, the Descemet's membrane, also known as the Lamina limitans posterior and the endothelium. Scale bar, 100µm. **C**, Iris with a musculus sphincter pupillae at the edge of the iris and a musculus dilatator pupillae more centrally. Scale bar, 100 µm.

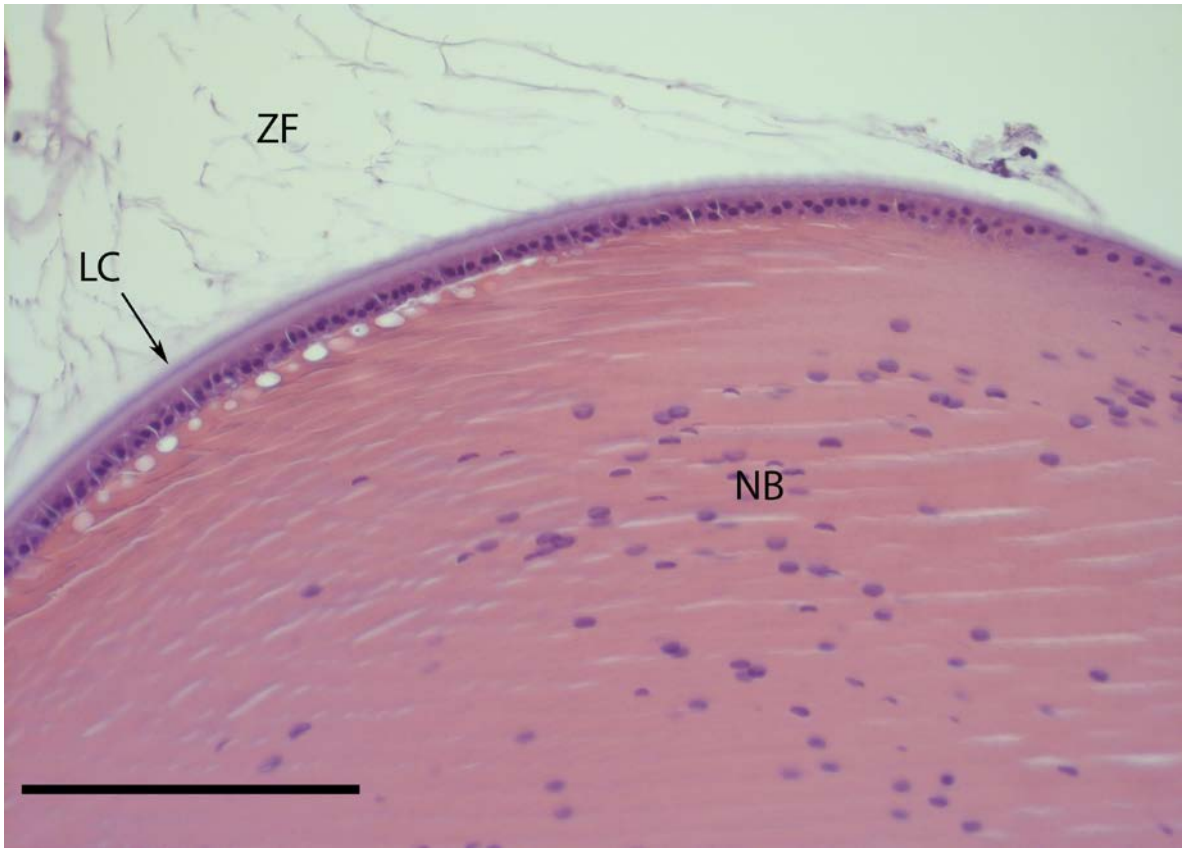

Figure 5 HE stained section of the lens.

Zonular fibres (ZF) connect the lens to the ciliary body. The thickness of the lens capsule (LC) decreased towards the convex posterior surface of lens. A typical nuclear bow (NB) was found beneath the capsule of the lens. Scale bar, 200 μm.

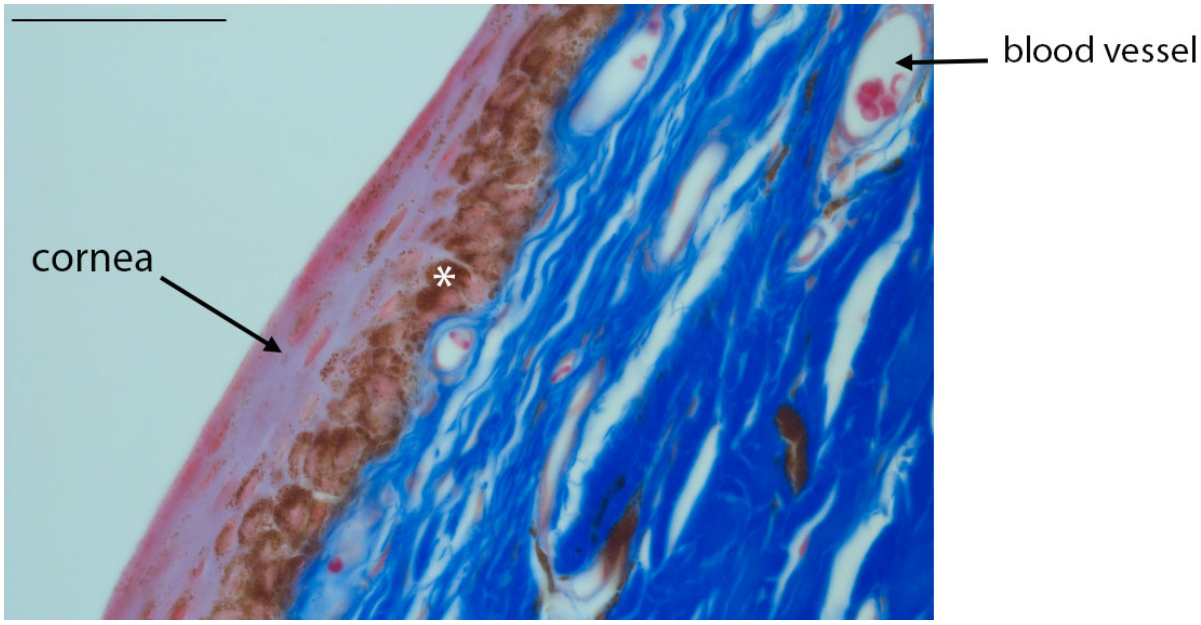

Figure 6 Azan stain of the peripheral cornea.

The pigmentation (asterisk) was most pronounced in the region of the sclero-corneal limbus. Scale bar, 50 µm.

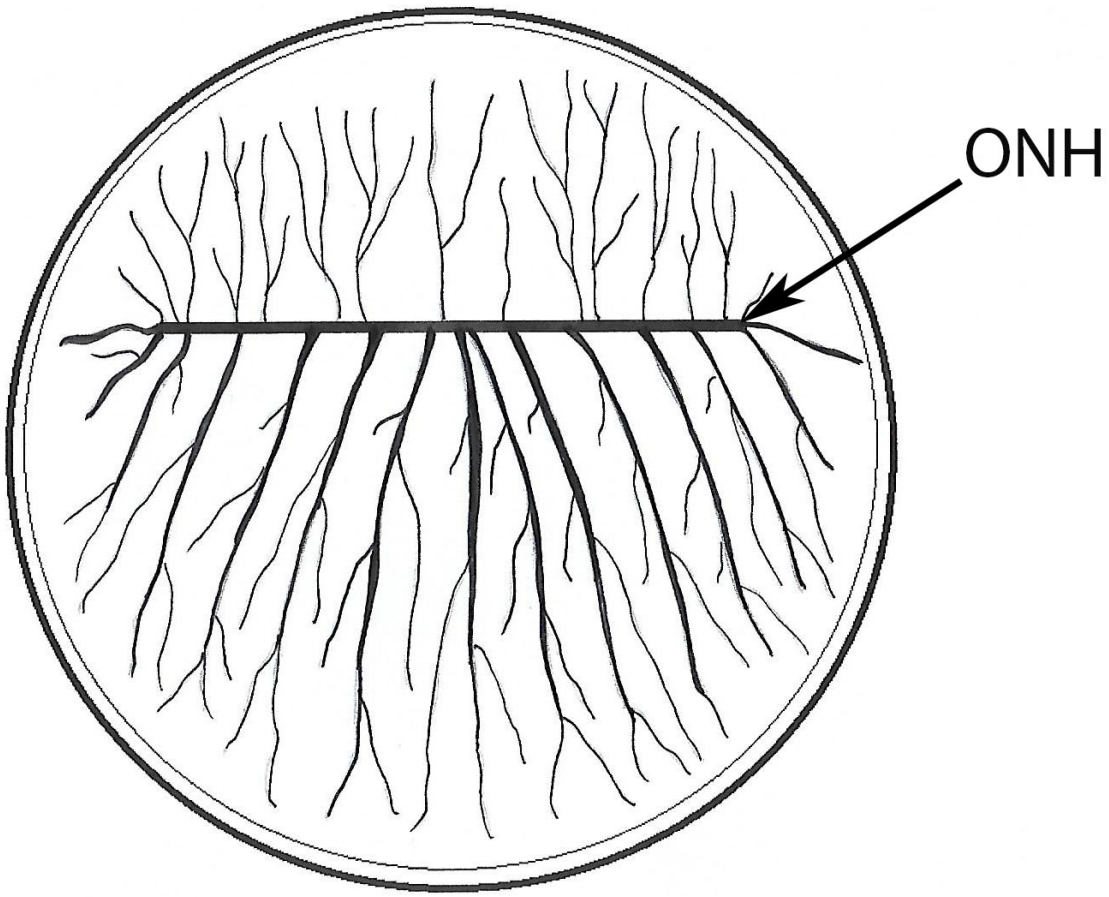

Figure 7 Vascularization of the eye of the alpine marmot.

The fundus shows a holangiotic distribution of the blood vessels. The vessels enter the retina at the optic nerve head (ONH).

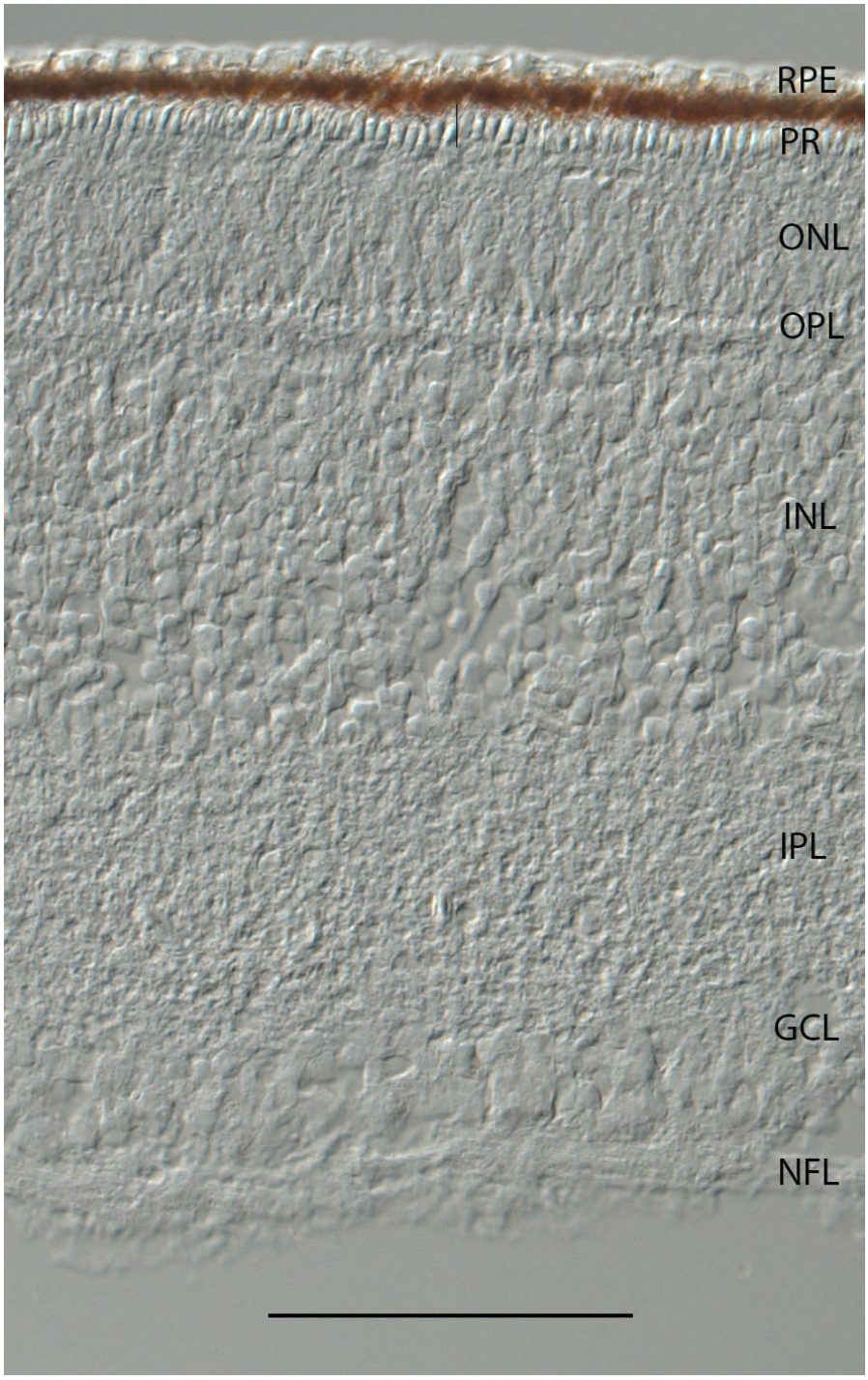

Figure 8 Gross morphology of the retina of the alpine marmot.

Differential interference contrast micrograph showing the layering of the retina. Retinal pigmented epithelium (RPE), photoreceptor inner segments (PR), outer nuclear layer (ONL), outer plexiform layer (OPL), inner nuclear layer (INL), inner plexiform layer (IPL), ganglion cell layer (GCL), nerve fibre layer (NFL). Scale bar, 100 µm.

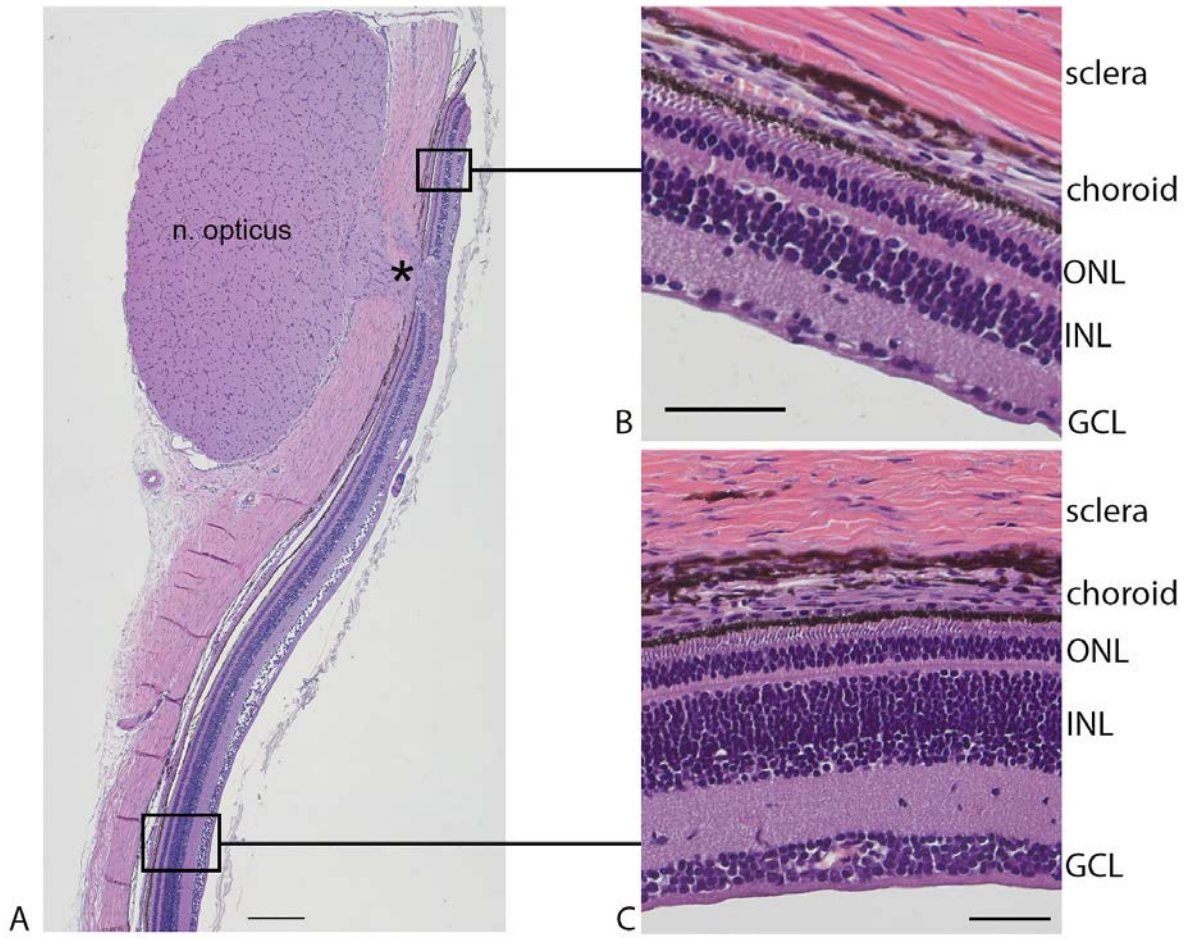

Figure 9 Microscopic structure of the retina, lamina cribrosa, and optic nerve.

A, Overview of the optic nerve, sclera, choroid, and the asymmetric retina. In the region of the lamina cribrosa (asterisk) the axons of the retinal ganglion cells (GCL) become myelinated and form the optic nerve. Scale bar, 200 µm. **B,** Dorsal retina. The retina is thinner dorsal to the optic nerve. Scale bar, 50 µm. **C**, Ventral retina. Retinal thickness increases threefold from dorsal to ventral. The inner nuclear layer (INL) ventral to the optic nerve measured twelve rows of nuclei. The dorsal outer nuclear layer (ONL) was one to two nuclei thick, the ventral ONL had three to four tiers of nuclei. Scale bar, 50 µm.

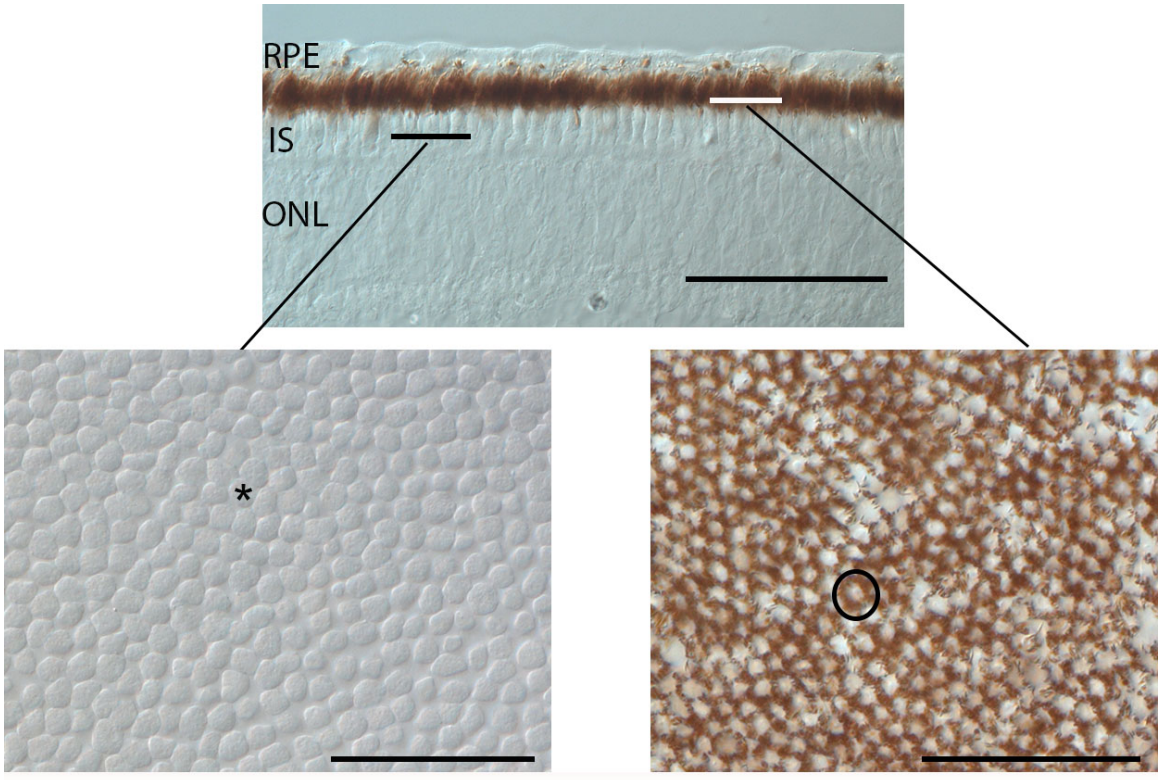

Figure 10 Microscopic view of the photoreceptors. A

Vertical cryostat section of the retina and the retinal pigment epithelium (RPE), demonstration the inner segments of the photoreceptors (IS) and the outer nuclear layer (ONL). B, The flat-mounted, unstained retina shows the retinal photoreceptor mosaic at the level of the inner segments (asterisk). C, The retinal photoreceptor mosaic at the level of the pigmented outer segments (example indicated by circle). Scale bar, 50 µm.

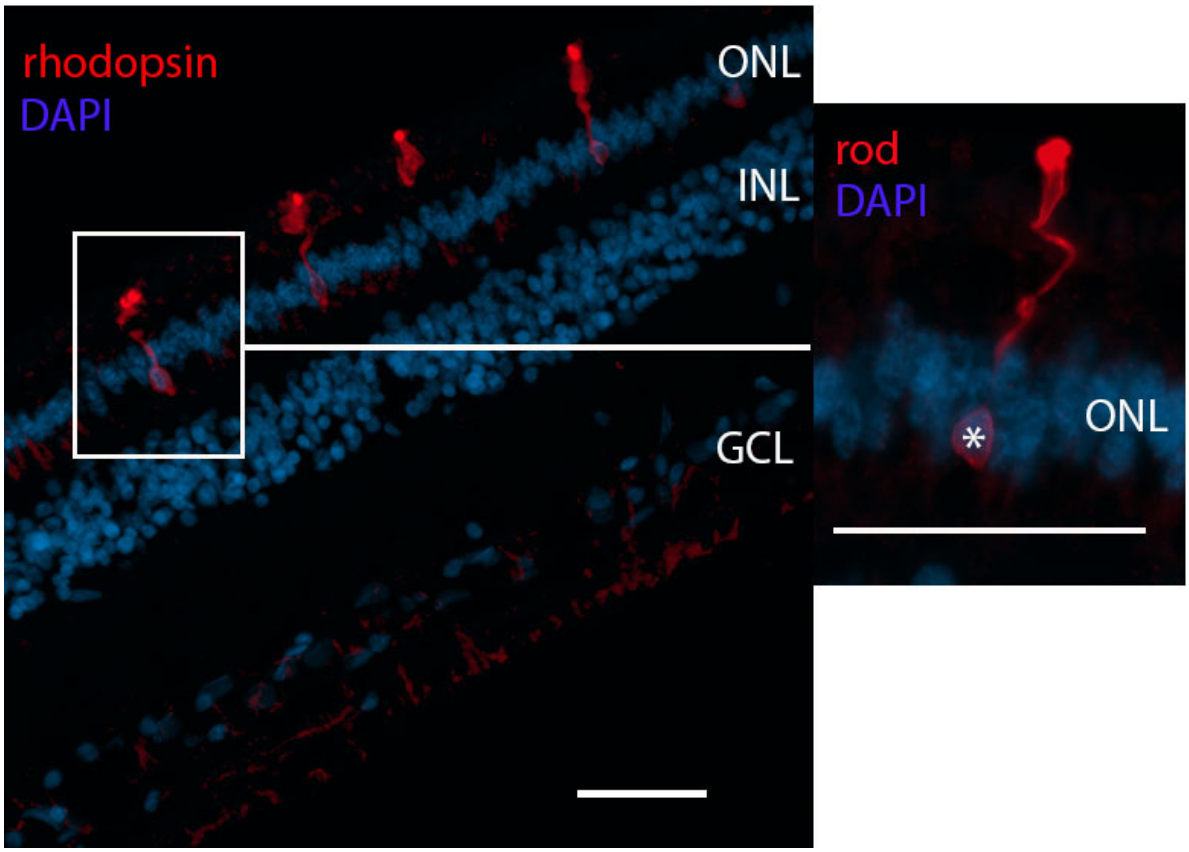

Figure 11 Immunostained vertical cryostat sections with rods identified by a rhodopsin specific antibody.

Nuclei labeled with DAPI. Rods (example boxed) are present in the retina of the alpine marmot but form a sparse population only. The majority of photoreceptors are cones. Their nuclei outnumber rod nuclei in the ONL but are not labeled by the anti-rhodopsin antibody. All rod somata (example shown in detail view, asterisk) are located in the inner part of the outer nuclear layer. Scale bar, 50 µm.

8. Abbreviations

AL	Axial length of the eye
a.s.l.	Above see level
CD	Corneal diameter of the eye
CL	Corneal limbus
CT	Corneal thickness
CD:ED	Relative corneal diameter with respect to the eye's equatorial diameter
CD:AL	Relative corneal diameter with respect to the eye's axial length
DAPI	4,6-diamidino-2-phenylindole
ED	Equatorial diameter
GCL	Ganglion cell layer
H&E	Hematoxylin and eosin stain
INL	Inner nuclear layer
IPL	Inner plexiform layer
L	lens
LC	Lens capsule
LD	Lens diameter
LD:ED	Relative lens diameter with respect to the eye's equatorial diameter
LT	Lens thickness
LT:AL	Relative lens thickness with respect to the eye's axial length
NaN_3	Sodium azide
NB	Nuclear bow
NBF	Neutral buffered formalin
NDS	Normal donkey serum
NFL	Nerve fibre layer
OCT	Optimal cutting temperature
ON	Optic nerve
ONH	Optic nerve head
ONL	Outer nuclear layer

OPL	Outer plexiform layer
OV	Musculus obliquus ventralis
P	Pupil
PBS	Phosphate buffered saline
PR	photoreceptor
RPE	Retinal pigment epithelium
R	Retina
RB	Musculus retractor bulbi
RD	Musculus rectus dorsalis
RM	Musculus rectus medialis
RV	Musculus rectus ventralis
RT	Room temperature
S	Sclera
SD	Standard deviation
UV	ultraviolet
ZF	Zonular fibres

9. References

Ahnelt PK. 1985. Characterization of the color related receptor mosaic in the ground squirrel retina. Vision research, 25 (11): 1557–1567. DOI 10.1016/0042-6989(85)90126-9.

Ahnelt PK, Kolb H. 2000. The mammalian photoreceptor mosaic-adaptive design. Progress in Retinal and Eye Research, 19 (6): 711–777. DOI 10.1016/S1350-9462(00)00012-4.

Arden GB, Tansley K. 1955. The spectral sensitivity of the pure-cone retina of the grey squirrel (*Sciurus carolinensis leucotis*). The Journal of Physiology, 127 (3): 592-602.1.

Arnold W. 1999a. Allgemeine Biologie und Lebensweise des Alpenmurmeltiers. Stapfia, (63): 1–20.

Arnold W. 1999b. Winterschlaf des Alpenmurmeltieres (*Marmota marmota*). Stapfia, (63): 43–56.

Bezuidenhout AJ, Evans HE. 2005. Anatomy of the woodchuck (*Marmota monax*). American Society of Mammalogists.

Bibikov DI. 1996. Die Murmeltiere der Welt. Marmota. Second ed. Magdeburg: Westarp-Wiss, 228.

Bonilha VL, Rayborn ME, Bhattacharya SK, Gu X, Crabb JS, Crabb JW, Hollyfield JG. 2006. The retinal pigment epithelium apical microvilli and retinal function. Advances in experimental medicine and biology, 572: 519–524. DOI 10.1007/0-387-32442-9_72 (accessed Jul 1, 2019).

Bornschein H. 1961. Zur Netzhautfunktion des Alpenmurmeltiers *Marmota marmota* (L.). Zeitschrift für vergleichende Physiologie, 44 (3): 262–267. DOI 10.1007/BF00298355.

Chou BR, Cullen AP. 1984. Spectral transmittance of the ocular media of the thirteen-lined ground squirrel (*Spermophilus tridecemlineatus*). Canadian Journal of Zoology, 62 (5): 825–830. DOI 10.1139/z84-120.

Cohen AI. 1964. Some Observations on the Fine Structure of the Retinal Receptors of the American Gray Squirrel. Investigative Ophthalmology and Visual Science, (3): 198–216.

Cullen CL. 2003. Normal ocular features, conjunctival microflora and intraocular pressure in the Canadian beaver (*Castor canadensis*). Veterinary Ophthalmology, 6 (4): 279–284. DOI 10.1111/j.1463-5224.2003.00307.x.

Douglas RH, Jeffery G. 2014. The spectral transmission of ocular media suggests ultraviolet sensitivity is widespread among mammals. Proceedings of the Royal Society B: Biological Sciences, 281 (1780). DOI 10.1098/rspb.2013.2995.

Duke-Elder S. 1958. System of ophthalmology. The Eye in Evolution. St. Louis: Mosby, 902.

Feldman JL, Phillips CJ. 1984. Comparative Retinal Pigment Epithelium and Photoreceptor Ultrastructure in Nocturnal and Fossorial Rodents: The Eastern Woodrat, *Neotoma floridana*, and the Plains Pocket Gopher, *Geomys bursarius*. Journal of Mammalogy, 65 (2): 231–245. DOI 10.2307/1381162.

Gur M, Sivak JG. 1979. Refractive state of the eye of a small diurnal mammal: the ground squirrel. American Journal of Optometry and Physiological Optics, 56 (11): 689–695. DOI 10.1097/00006324-197911000-00004.

Hains PG, Simpanya MF, Giblin F, Truscott RJW. 2006. UV filters in the lens of the thirteen lined ground squirrel (*Spermophilus tridecemlineatus*). Experimental Eye Research, 82 (4): 730–737. DOI 10.1016/j.exer.2005.09.014.

Hollenberg MJ, Bernstein MH. 1966. Fine structure of the photoreceptor cells of the ground squirrel (*Citellus tridecemlineatus tridecemlineatus*). The American Journal of Anatomy, 118 (2): 359–373. DOI 10.1002/aja.1001180204.

Hughes A. 1977. The Visual System in Vertebrates. Berlin, Heidelberg: Springer Berlin Heidelberg, Online-Ressource.

Kay RF, Kirk EC. 2000. Osteological evidence for the evolution of activity pattern and visual acuity in primates. American Journal of Physical Anthropology, 113 (2): 235–262. DOI 10.1002/1096-8644(200010)113:2<235:AID-AJPA7>3.0.CO;2-9.

Kirk EC. 2004. Comparative morphology of the eye in primates. The anatomical record. Part A, Discoveries in molecular, cellular, and evolutionary biology, 281 (1): 1095–1103. DOI 10.1002/ar.a.20115.

Kirk EC. 2006. Eye morphology in cathemeral lemurids and other mammals. Folia primatologica; International Journal of Primatology, 77 (1-2): 27–49. DOI 10.1159/000089694 (accessed Aug 16, 2019).

König HE, Liebich H-G, Aurich C, Hrsg. 2014. Veterinary anatomy of domestic mammals. Textbook and colour atlas; with 53 tables. Sixthth, rev. and extended ed. Stuttgart, New York, NY: Schattauer, 804.

Kruckenhauser L, Haring E, Arnold W, Pinsker W. 1999. Die Phylogenie der Gattung *Marmota* (Rodentia, Sciuridae): Ein Stammbaum auf der Basis von DNA-Sequenzdaten. Stapfia, (63): 169–176.

Kryger Z, Galli-Resta L, Jacobs GH, Reese BE. 1998. The topography of rod and cone photoreceptors in the retina of the ground squirrel. Visual Neuroscience, 15 (4): 685–691. DOI 10.1017/S0952523898154081.

Kuester LA, Komáromy AM, Brooks DE, Lewis PA, Bennett F, Chisholm M. 2004. Optic nerve head morphology of the Eastern gray squirrel, *Sciurus carolinensis*. Veterinary Ophthalmology, 7 (3): 169–173. DOI 10.1111/j.1463-5224.2004.04017.x.

Long KO, Fisher SK. 1983. The distributions of photoreceptors and ganglion cells in the California ground squirrel*, Spermophilus beecheyi*. The Journal of Comparative Neurology, 221 (3): 329–340. DOI 10.1002/cne.902210308.

Meekins JM, Eshar D, Rankin AJ, Henningson JN. 2016. Clinical and histologic description of ocular anatomy in captive black-tailed prairie dogs (*Cynomys ludovicianus*). Veterinary Ophthalmology, 19 (2): 110–116. DOI 10.1111/vop.12266.

Merriman DK, Sajdak BS, Li W, Jones BW. 2016. Seasonal and post-trauma remodeling in cone-dominant ground squirrel retina. Experimental eye research, 150: 90–105. DOI 10.1016/j.exer.2016.01.011.

Mulisch M, Welsch U, Hrsg. 2015. Romeis Mikroskopische Technik. Nineteenth. Auflage. Berlin, Heidelberg: Springer Spektrum, 611.

Müller B, Peichl L. 1989. Topography of cones and rods in the tree shrew retina. The Journal of Comparative Neurology, 282 (4): 581–594. DOI 10.1002/cne.902820409.

Ollivier FJ, Samuelson DA, Brooks DE, Lewis PA, Kallberg ME, Komáromy AM. 2004. Comparative morphology of the tapetum lucidum (among selected species). Veterinary Ophthalmology, 7 (1): 11–22.

Peichl L. 2005. Diversity of mammalian photoreceptor properties: adaptations to habitat and lifestyle? The anatomical record. Part A, Discoveries in molecular, cellular, and evolutionary biology, 287 (1): 1001–1012. DOI 10.1002/ar.a.20262.

Peichl L, Kaiser A, Rakotondraparany F, Dubielzig RR, Goodman SM, Kappeler PM. 2016. Diversity of photoreceptor arrangements in nocturnal, cathemeral and diurnal Malagasy lemurs. The Journal of Comparative Neurology, 527 (1): 13–37. DOI 10.1002/cne.24167.

Peichl L, Künzle H, Vogel P. 2000. Photoreceptor types and distributions in the retinae of insectivores. Visual Neuroscience, 17 (6): 937–948. DOI 10.1017/s0952523800176138.

Rocha FAdF, Ahnelt PK, Peichl L, Saito CA, Silveira LCL, Lima SMA de. 2009. The topography of cone photoreceptors in the retina of a diurnal rodent, the agouti (*Dasyprocta aguti*). Visual Neuroscience, 26 (2): 167–175. DOI 10.1017/S095252380808098X.

Rochon-Duvigneaud A. 1930. Auge von *Marmotta*. Verh. 13. Internat. Kongr. Ophthalm., 1: 319.

Rodriguez-Ramos Fernandez J, Dubielzig RR. 2013. Ocular comparative anatomy of the family Rodentia. Veterinary Ophthalmology, 16 Suppl 1: 94–99. DOI 10.1111/vop.12070.

Schaepdrijvers LDE, Simoens P, Lauwres H, Geest JPD. 1989. Retinal vascular patterns in domestic animals. Research in Veterinary Science, 47 (1): 34–42. DOI 10.1016/S0034-5288(18)31228-1.

Szél Á, Röhlich P. 1988. Four photoreceptor types in the ground squirrel retina as evidenced by immunocytochemistry. Vision Research, 28 (12): 1297–1302. DOI 10.1016/0042-6989(88)90060-0.

Türk A, Arnold W. 1988. Thermoregulation as a limit to habitat use in alpine marmots (*Marmota marmota*). Oecologia, 76 (4): 544–548. DOI 10.1007/BF00397867.

Walls GL. 1942. Vertebrate eye and its adaptive radiation. Bloomfield Hills, Mich.: Cranbrook Institute of Science.

Wässle H. 2004. Parallel processing in the mammalian retina. Nature reviews. Neuroscience, 5 (10): 747–757. DOI 10.1038/nrn1497.

West RW, Dowling JE. 1975. Anatomical evidence for cone and rod-like receptors in the gray squirrel, ground squirrel, and prairie dog retinas. The Journal of Comparative Neurology, 159 (4): 439–460. DOI 10.1002/cne.901590402.